Electrophoretic deposition of hydroxyapatite

I. ZHITOMIRSKY, L. GAL-OR
Israel Institute of Metals, Technion-Israel Institute of Technology, Haifa, 32000 Israel

Hydroxyapatite powders were prepared by a chemical precipitation method and electrophoretically deposited on Ti6Al4V surgical alloy substrates. The powders were characterized by scanning electron microscopy (SEM), X-ray diffraction (XRD), particle size distribution and zeta potential measurements. Prior to electrophoretic deposition, anodic films were obtained on Ti6Al4V and studied by the Auger method. It was established that experimental conditions of powder preparation, electric field and stirring have a significant influence on suspension stability and deposit morphology. The deposition yield was studied at various deposition durations and applied voltages. Sintered coatings were studied by SEM and XRD.

1. Introduction

Hydroxyapatite $Ca_{10}(PO_4)_6(OH)_2$ (HA) is an important material for bone and tooth implants [1–3], as its chemical composition is similar to that of bone tissue. Owing to the inferior mechanical properties of HA, significant research activity has been associated with the development of HA coatings and composites. The importance of HA coatings and composites for biomedical applications has motivated the further development of processing technologies. The interest in electrophoresis for biomedical applications [4–10] stems from a variety of reasons such as the possibility of deposition of stoichiometric, high purity material to a degree not easily achievable by other processing techniques and the possibility of forming coatings and bodies of complex shape as well as HA lining of metal fibre networks [5]. A new wave of interest in electrophoretic technology is concerned with the use of submicrometre ceramic particles. Electrophoretic deposition of submicrometre powders offers advantages in fabrication of ceramic coatings and bodies with dense packing, good sinterability and homogeneous microstructure [11, 12]. One of the important capabilities provided by fine particle electrophoresis is the ability to achieve ceramic particle impregnation into a porous substrate [13] and composite consolidation.

It is now well established that the state of agglomeration of ceramic powders is an important factor in controlling the sintering behaviour. Agglomerate-free structures made from close-packed fine particles can be densified at lower sintering temperatures. An important advantage of electrophoretic processing is that agglomerates can be separated by pre-sedimentation [11]. Moreover, owing to the insulating properties of the deposit, the electric field provides a higher deposition rate in defect regions, resulting in better packing and uniformity of the deposit.

Fine HA particles can easily be precipitated via a wet chemical method [14, 15], however, they exhibit a significant tendency to agglomeration. A significant problem is associated with the use of additives because of the risk of contamination and the low chemical stability of HA. However, additives are necessary in order to obtain stable suspensions and to achieve the desired level of electrophoretic mobility [9, 10, 16].

Another problem is water adsorption. As previously pointed out [5], adsorbed water interferes with electrophoretic transport and therefore electrophoretic deposition of non-calcined HA powders was not achieved. The choice of a suitable solvent is important for electrophoretic deposition. Organic liquids are preferable to water since electrophoretic deposition in water is accompanied by significant gas evolution.

In this work, the experimental results of a study of electrophoretic deposition of HA powders, performed in isopropyl alcohol as a suspension medium, are reported.

2. Experimental procedure

The procedure for preparation of stoichiometric HA was based on that previously described [14, 15]. As starting materials commercially guaranteed $Ca(NO_3)_2 \cdot 4H_2O$ (Aldrich), $(NH_4)_2HPO_4$ (Merck) and NH_4OH (Palacid) were used. Precipitation was performed at a temperature of 70 °C by the slow addition of a 0.6 M ammonium phosphate solution into a 1.0 M calcium nitrate solution. The pH of the solutions was previously adjusted to 11 by addition of NH_4OH. Stirring was performed for 24 h at 70 °C and 48 h at room temperature.

Two different HA powders were prepared: HA1 powder was prepared by washing the precipitate obtained with water and drying at 60 °C for 48 h. For HA2 preparation, the precipitate obtained was washed with water and finally with isopropyl alcohol and stored in a moisture-free atmosphere for three weeks. The weight of HA2 was controlled and no weight change was observed after this period. After milling in an agate mortar the HA1 and HA2 powders obtained were used for the study.

0957–4530

The stoichiometry of the HA obtained was proven by chemical analysis. The HA powders were characterized with an X-ray diffractometer (Phillips, model PW-1820) operated at 40 kV and 40 mA using monochromatized CuK_{α} radiation at a scanning speed of 0.3 degree/min. Average crystallite sizes were calculated by means of X-ray line broadening measurements using a commercially available computer program. The particle size distribution of HA powders was studied by a laser scattering method using a computerized inspection system (GALAI-CIS-1).

Suspensions for electrophoretic experiments were prepared by ultrasonic agitation of HA powders in isopropyl alcohol. The HA concentration in suspensions was 30 g/l. Zeta potential and electrophoretic mobility were studied using a Laser Zee Meter (Pen Kem, model 501). Electrophoretic deposition experiments were performed at various voltages ranging from 10 to 200 V, deposition times were 10 s to 5 min. The distance between the electrodes was 15 mm. The current density was recorded during the deposition process. The deposition process has been studied at various deposition times and voltages on Ti6Al4V alloy substrates. Specimens of Ti6Al4V surgical alloy were rinsed with acetone in an ultrasonic bath, washed with distilled water and then used for electrophoretic deposition. For sintering experiments, HA coatings were also obtained on anodized substrates. Anodization of specimens was performed in 8% H_3PO_4 solution. The electrochemical anodization cell included the anodic substrate centred between two parallel platinum counterelectrodes. The current densities ranged from 5 to 20 mA/cm^2 and anodization durations were 1–10 min. After rinsing in water and drying in air these specimens were used as substrates for electrophoretic experiments. The anodic films were studied by a scanning Auger microscope (Perkin–Elmer, PHI model 590A).

The coatings obtained were dried in air in an oven at 60 °C for 2 h and then sintered in a vacuum furnace (1.33×10^{-4} Pa) at 930 °C for 2 h. Coating morphology was studied by scanning electron microscopy (Jeol, model JSM-840).

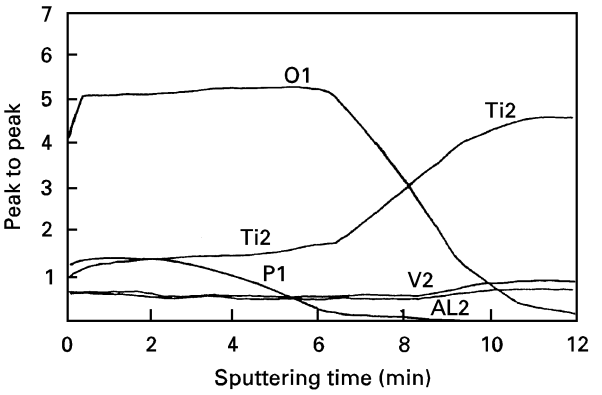

Figure 1 Auger depth profile of TiAlV substrate after anodization (sputtering rate 150 A/min).

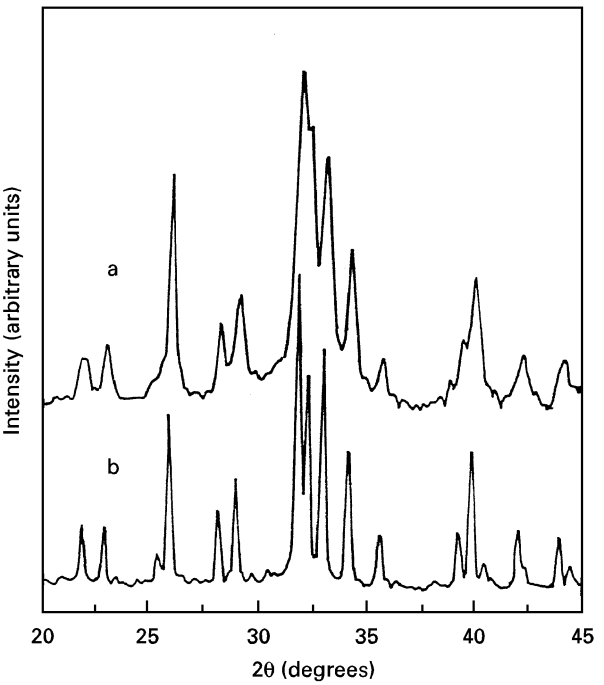

Figure 2 X-ray diffraction patterns of HA2 (a) as prepared and (b) calcined at 1100 °C.

3. Experimental results

Prior to electrophoretic deposition, Auger studies of the anodic films on the TiAlV substrates were performed. The Auger data show that anodic films include phosphorus in addition to oxygen and alloy components. A typical Auger depth profile for the TiAlV specimens after anodization is shown in Fig. 1. As seen in Fig. 1, at 900 A the oxygen peak O1 (at 512 eV) begins to decrease, correspondingly the titanium peak Ti2 (at 418 eV) begins to increase signifying the beginning of the transition to the alloy. However, a significant tail is seen in the depth profile for oxygen, and for this reason the evaluation of film thickness presents difficulties. In light of the above, film thickness was assumed to be the thickness corresponding to a 50% decrease in the height of the oxygen peak O1. It was established that the film thickness defined by this manner was in the region of $\sim$150 nm for the anodic films obtained under the experimental conditions described above.

Typical examples of X-ray diffraction patterns of as-prepared HA powders and of HA powders after thermal treatment at 1100 °C in air for 2 h are shown in Fig. 2. XRD data show a crystalline structure for non-calcined powders, however, corresponding X-ray peaks are broadened due to the fine size of the crystallites. The average crystalline dimension obtained from XRD patterns of as-prepared HA2 powders was found to be 55 nm. The XRD peaks of HA became sharper after thermal treatment. It was established that HA1 powders were highly agglomerated, and agglomerate size was up to several micrometres as seen from the particle size distribution presented in Fig. 3. In contrast, particle size distribution measurements for HA2 powders revealed particle sizes in the submicrometre range. These results are in a good agreement with the results of SEM examinations of corresponding powders.

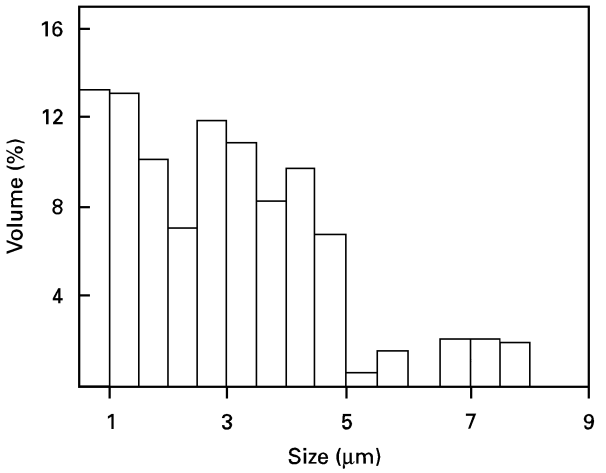

Figure 3 Particle size distribution for dried HA1 powders.

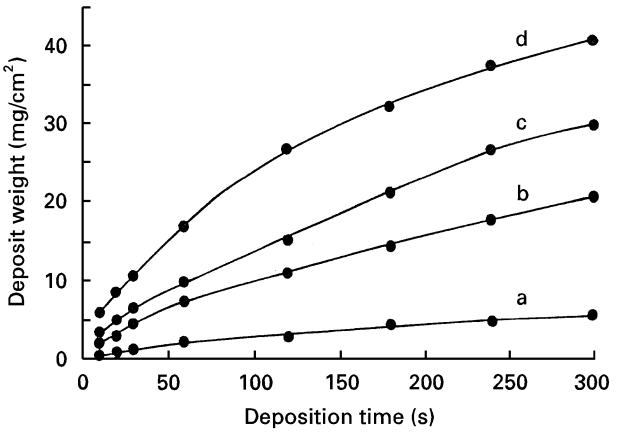

Figure 4 Weight of deposited HA2 versus deposition time at different applied voltages: (a) 10 V; (b) 50 V; (c) 100 V; (d) 200 V.

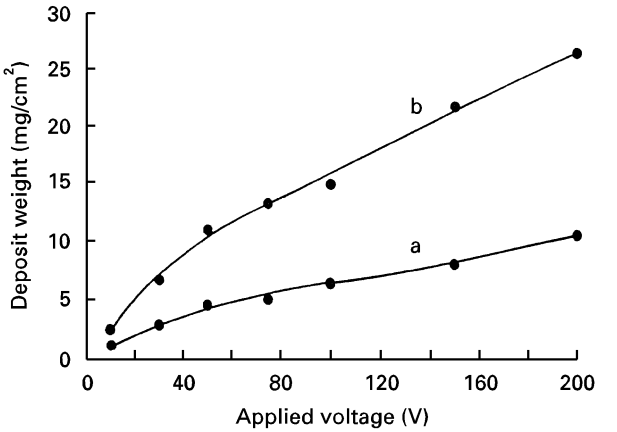

Figure 5 Weight of deposited HA2 versus applied voltage for different deposition durations: (a) 30 s; and (b) 120 s.

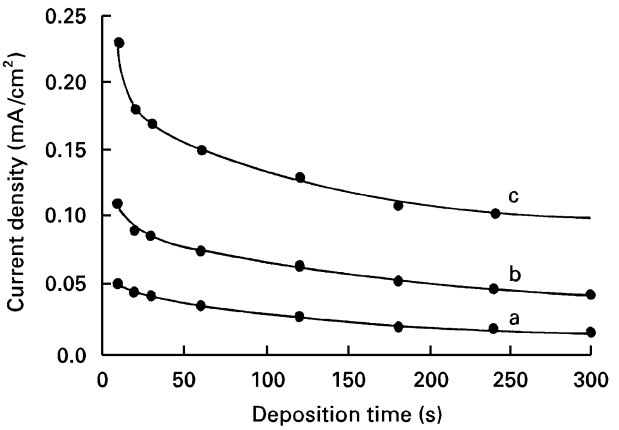

Figure 6 Current density versus deposition time for deposition of HA2 at different applied voltages: (a) 50 V; (b) 100; (c) 200 V.

Electrophoretic experiments revealed that HA particles were positively charged and moved towards the cathode under the applied field. It should be noted that electrophoretic deposition was achieved for both fresh HA1 and HA2 suspensions. Zeta-potential measurements for HA2 powders revealed an increase in zeta-potential value from $+22$ to $+30$ mV during the first 3 days; after this ageing period it remained nearly constant.

It is important to note that stable suspensions are necessary for electrophoretic deposition experiments. However, ultrasonically treated HA1 suspensions exhibited significant settling after several tens of minutes. In contrast, HA2 suspensions were found to be stable for 1–2 days. It was also established that in the case of HA2 suspensions, which contained submicrometre particles, magnetic stirring was found to have a detrimental effect on suspension stability and led to relatively fast settling when stirring was interrupted. The electric field also has an adverse effect on the HA2 suspension stability. Passing an electric current through the suspension during electrodeposition also brought about significantly faster settling, especially at deposition voltages higher than 100 V.

In order to study deposit weights obtained at various experimental conditions HA suspensions were ultrasonically treated immediately before electrophoretic deposition. Deposit weights for HA1 and HA2 obtained on cathodic TiAlV alloy substrates were found to increase with increase of voltage and deposition time. Figs 4 and 5 show the weight of the coating per unit surface area as a function of deposition time and applied voltage for experiments performed with HA2 suspensions. As seen in Fig. 4, slopes of the curves decrease with time, indicating a decrease of the deposition rate. Correspondingly, the deposition current decreased with time as shown in Fig. 6. The microstructures of HA1 coatings were strongly influenced by the electric field. An interesting observation regarding film microstructures is the difference in particle size of the deposits obtained at various voltages. SEM observations have shown that HA1 deposits obtained at 200 V included particles of various dimensions ranging up to several micrometres (Fig. 7a, b). This is in good agreement with the particle size distribution shown in Fig. 3. SEM examinations of particle sizes of HA1 deposits obtained at lower voltages have shown preferable deposition of fine particles. As seen in Fig. 7c the maximum particle size in a deposit obtained at 20 V is about 1 micrometre and the deposit includes a significant amount of very fine particles. As expected, suspension presedimentation was found to have a significant effect on the particle size of deposits. Presedimentation allowed the removal of

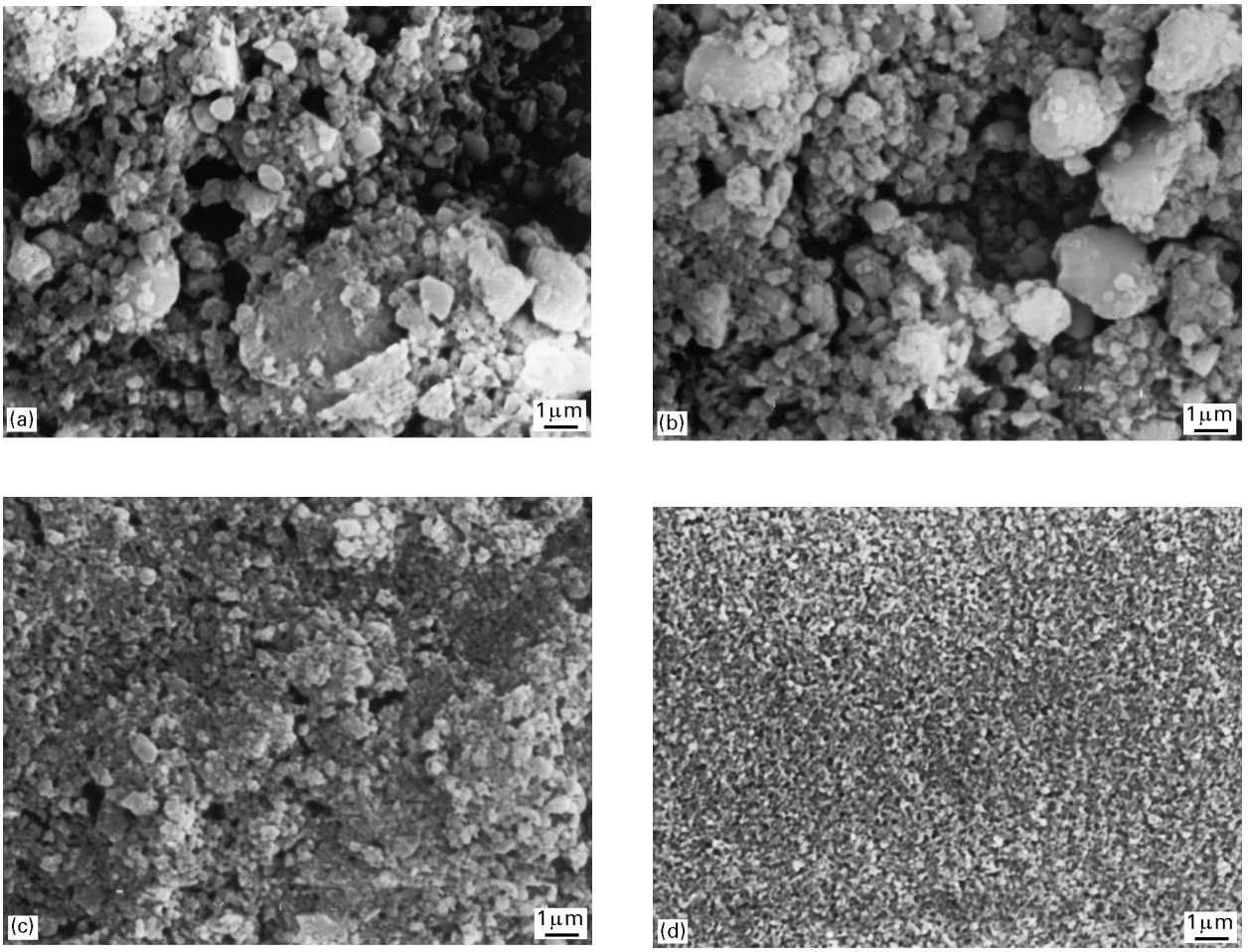

Figure 7 SEM pictures of the HA1 deposits on TiAlV substrates at different applied voltages: (a, b) 200 V; (c) 20 V; (d) 10 V (a, b, c—without presedimentation, d—1 h presedimentation).

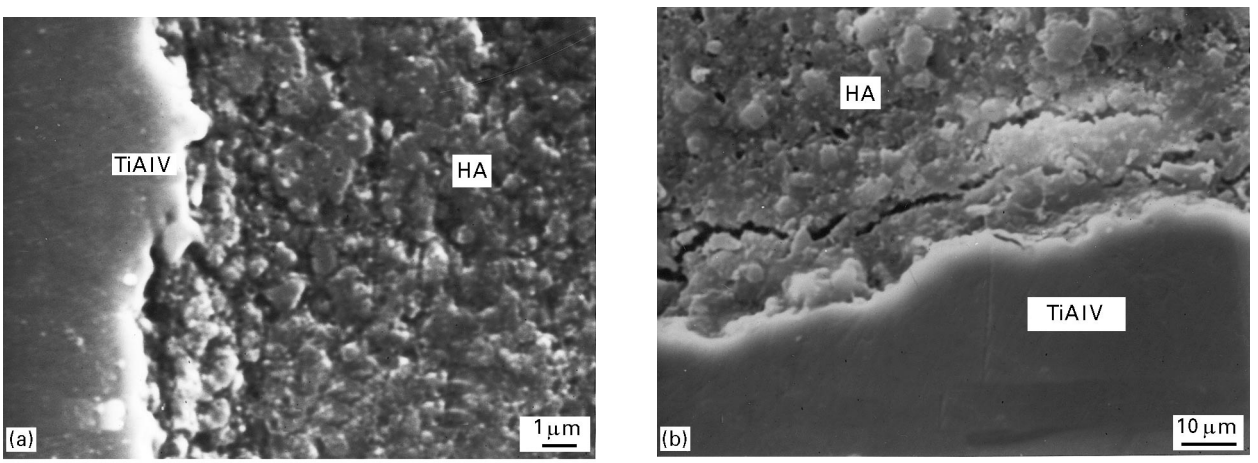

Figure 8 SEM pictures of sintered HA coatings on TiAlV substrates.

agglomerates from suspensions and as a result, the deposits obtained consisted of finer particles. It was established that by use of presedimentation and low voltages it was possible to obtain deposits which consisted only of submicrometre particles. As seen in Fig. 7d after 1 h of presedimentation the deposit obtained at 10 V includes only very fine particles on a submicrometre scale. Another microstructural feature was the higher coatings porosity obtained at higher voltages. As seen in Fig. 7b pores of up to several micrometres were observed in the deposits. This porosity is speculated to be a consequence of gas evolution. In contrast, deposits obtained at 20 V included (Fig. 7c) significantly smaller pores and exhibited a denser packing. Deposits obtained at 10 V after presedimentation showed a homogeneous microstructure with porosity on a submicrometre scale (Fig. 7d). HA2 coatings obtained at voltages below 50 V exhibited morphologies similar to that shown in Fig. 7d.

Sintered HA2 coatings were relatively dense and adherent to the substrate. In contrast, HA1 coatings can easily be removed from the substrates. Fig. 8a, b

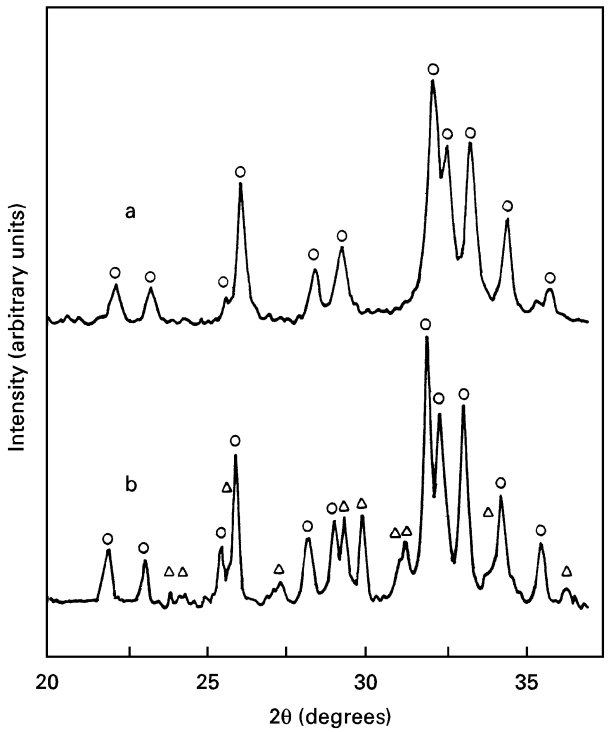

Figure 9 X-ray diffraction patterns of HA2 coating on TiAlV substrtate: (a) green deposit; and (b) deposit sintered at 930 °C; ○-HA, △-TTCP.

shows HA2 coatings of TiAlV substrates after sintering. SEM pictures exhibit partial densification of coatings, as indicated by a decrease of porosity, particle coalescence and interparticle neck formation. Cracks were also observed in coatings (Fig. 8b) near coating–substrate interface.

X-ray diffraction patterns of a green deposit and of one sintered at 930 °C are shown in Fig. 9. The X-ray diffraction pattern of the green coating shows well–defined peaks of HA. Results of X-ray studies of the sintered coatings did not lead to any radically new information with respect to that described by Ducheyne *et al.* [5]. Reflections of tetracalciumphosphate (TTCP) were observed in the sintered coatings in addition to HA reflections. However, the relative intensity of TTCP reflections decreased with increase of anodic film thickness.

4. Discussion

The above experimental data suggest that fresh (non-calcined) HA powders can be electrophoretically deposited on Ti alloy substrates. This is in contrast to literature data [5, 9], according to which, no electrophoretic deposition of fresh powders was achieved. As suggested by Ducheyne *et al.* [5], adsorbed water in non-calcined powders prevented electrophoretic deposition. Furthermore, hydrolysis of water resulted in high current densities.

Results of the present study indicate that in experiments performed with fresh HA2 powders, the observed current densities were, by several orders of magnitude, lower than those for non-calcined stoichiometric HA studied by Ducheyne *et al.* [5]. However, it is noteworthy that the deposit weights obtained for fresh HA2 powders were comparable to those for the calcined powders studied in [5] under the same conditions of deposition process (electric field, time, concentration of HA particles). As in other research work [9, 17], variation of the initial zeta-potential with time was observed in the case of HA2 powders, however, it should be mentioned that, in contrast to experiments performed with aqueous suspensions [17], the ageing effects did not result in change of sign of zeta-potential. The results of this work indicate that the electrophoretic behaviour of fresh HA powders is quite different from that described in [5, 9]. This can be attributed to differences in surface characteristics resulting from different conditions of powder preparation. Comparative data of electrophoretic behaviour of zirconia powders prepared at various experimental conditions [18] can be invoked to support this explanation.

As a first approximation the deposit weight W in the electrophoretic process can be described by the following equation:

$$W = C\mu Ut/d \tag{1}$$

where C and μ are particle concentration and mobility, respectively, $U = U_{ap} - U_{dep}$ where U_{ap} = applied voltage, U_{dep} = voltage drop in deposit, t is deposition time, and d is distance between electrodes. The electrophoretic mobility can be determined [19] from the Smoluchowski equation:

$$\mu = \zeta\varepsilon/4\pi\eta \tag{2}$$

where ζ = zeta potential, ε = dielectric constant and η = viscosity of the medium.

In accordance with Equation 1 deposit weight was found to increase with increase of deposition time and voltage. Increase of coating thickness during the deposition process brings about the increase of voltage drop in the deposit. Correspondingly, a decrease in deposition rate with time was observed.

Electron microscopic investigations have shown that the microstructures of deposits were strongly influenced by powder characteristics and by the magnitude of electric field. As expected, agglomerate content in the deposited material can be decreased by use of presedimentation.

Experiments performed with HA1 powders have also shown that the influence of the electric field on deposit morphology needs to be addressed. The influence of the electric field on the electrophoretic deposition process has been discussed in the literature [20–26]. The electric field drives the particles towards the electrode and exerts a pressure on the deposited layer. From this point of view a higher electric field should result in higher deposit density. However, no appreciable variation of green density with deposition voltage was observed in [26]. According to [12] the increase in green density with voltage was observed only at relatively low voltages and deposit thicknesses. The use of high voltages has the advantage of smaller deposition times and higher deposit thicknesses. It should be noted that in the case of relatively large particles (more than 1 μm) stirring of the suspension is

usually performed in order to prevent settling [24]. In this respect, higher voltages and smaller deposition times were found to be preferable [24], because shorter deposition times allow deposition without stirring. However, higher voltages usually result in significant hydrogen evolution at the cathode which, in turn, increases the porosity of the deposit [23]. According to [25] more adherent and continuous coatings with less cracking can be obtained at lower voltages. On the other hand it was pointed out [20, 21] that a certain value of electric field is necessary in order to overcome interparticle interactions and to allow particles to bond to the substrate.

For electrophoretic velocity ν Equation 2 takes the form:

$$\nu = \zeta E \varepsilon / 4\pi\eta \tag{3}$$

where $E = U/d$ potential gradient. According to [22, 27, 28]:

$$\nu \propto QE/r\eta \tag{4}$$

where Q and r are charge and radius of particles, respectively.

Particles with different Q/r ratios have different electrophoretic mobilities and segregation effects can be expected in the electrodeposition process [22]. According to [27, 28] fine particles should be deposited preferably. In spite of expectations no appreciable segregation effect was observed in [23]. In contrast, preferable deposition of fine particles was observed [26].

SEM observations of HA1 green deposits have shown that higher electric fields bring about porosity of the deposit. This is in agreement with [23]. Experiments performed with HA1 powders also exhibited finer particle size of green deposits obtained at lower electric fields. In this context, it should be mentioned that a similar effect was also observed in our experiments performed with submicrometre alumina powders. Results of this study will be published soon.

Another point to be discussed is the influence of the electric field and stirring on the stability of HA2 suspensions. It is an important observation that electric field as well as stirring initiate sedimentation and thus adversely affect the suspension stability. It can be supposed that the presence of an electric field and stirring result in interaction of fine particles, their aggregation and subsequent sedimentation. It should be mentioned that particle aggregation in strong electric fields has been described in the literature [29]. Particle aggregation and sedimentation induced by the electric field can be considered as an additional reason for the decrease of deposition rate with time. Indeed, particle sedimentation results in a decrease of suspension concentration and, in accordance with Equation 1, should result in a decrease of the deposition rate. It is clear that electric-field-induced particle sedimentation decreases the amount of fine particles in the suspension and in the deposit, this effect being more distinct in higher electric fields. In contrast, at lower fields the concentration of fine particles, and correspondingly their deposition rate, become higher. As a result preferable deposition of fine HA1 particles was observed. This finding is in line with the results of Andrews *et al.* [26]. It should be noted that the ceramic powders used in numerous works on electrophoretic deposition [20–26] had different distributions of particle sizes. It is reasonable to expect that electrophoretic phenomena have distinctive features for relatively large particles (several micrometres) and for particles on a submicrometre or nanometre scale. In light of the above it can be concluded that when the influence of the electric field on the electrophoretic process is studied particle size distribution should also be taken into consideration.

At this point it is important to mention that centrifuging of colloidal suspensions brings about particle agglomeration and sedimentation [30]. It is not surprising, therefore, that HA2 suspensions consisting of submicrometre particles exhibited a tendency to rapid settling when stirring was performed. In the centrifuging technique used by Pliskin and Conrad [30] for coating development, aggregation and sedimentation were influenced by particle size, dielectric constant and viscosity of the suspending medium.

As stated above, HA1 and HA2 deposits exhibit different sintering behaviour. It is expected that the reduction of particle size in HA2 powders with respect to that in HA1 powders should result in high reactivity of HA2 powders. Indeed, according to [31, 32] the densification rate depends inversely on the fourth power of particle size in accordance with the relation:

$$\partial\rho/\partial t = A\gamma_s\Omega/kT\{D_b\delta_b/d^4 + D_v/d^3\} \tag{5}$$

where ρ is the density, γ_s is the surface free energy, Ω is the atomic volume, D_b and D_v are the grain boundary and bulk diffusion coefficients, respectively, and δ_b is the grain boundary thickness. As pointed out [32], reduction of particle sizes from micrometric to nanometric scale should increase densification rate by several orders of magnitude. Studies carried out by Best and Bonfield have shown a significant influence of HA particle morphology on sintering behaviour [33]. According to [34] sol–gel derived HA coatings were partially sintered at a temperature as low as 900 °C. It is apparent that the observed partial densification of the HA2 powders at 930 °C observed in this work can be attributed to the submicrometre particle sizes of HA2 powders.

The phase transformations in HA sintered on Ti and alloy substrates are amply documented in available literature [4–6]. Sintering of the coating must be performed below the $\alpha + \beta \rightarrow \beta$ transition temperature for the Ti–6% Al–4% V substrate (975 °C). The use of this alloy requires a high degree of vacuum. On the other hand, HA ceramic was found to achieve maximum density above 1100 °C [14]. Stoichiometric HA is stable in vacuum at temperatures below 1000 °C, however, Ti initiates decomposition of HA [4–6]. Vacuum sintering of HA on the alloy substrate results in phase transformation. It was established [6] that during the sintering of HA coatings, diffusion of phosphorus into the substrate takes place and as a result HA partially decomposes to form TTCP with a higher Ca/P ratio.

The results of our X-ray study of sintered coatings are in good agreement with the results of [5],

according to which the HA coating after sintering at 930 °C partially decomposed to form TTCP. One way to alleviate the problem of HA decomposition is formation of titanium oxide layers [5, 6]. In this work an anodization process has been utilized for the formation of the oxide layer. The incorporation of phosphorus into the oxide layer during anodization is in good agreement with previous work [35]. It can be expected that a P-containing oxide layer will provide decreased compositional changes in HA coatings which arise from the diffusion of P into the metal substrate. Further experiments are underway to elucidate the role of anodic layer thickness and phosphorus content on phase transformation in HA layers neighbouring the coating alloy interface.

5. Conclusions

Chemically precipitated hydroxyapatite powders were electrophoretically deposited on TiAlV alloy substrates. For substrates subjected to anodization experiments the anodic films were characterized by Auger spectrography. The Auger data show that anodic films included phosphorus in addition to oxygen and alloy components. It was established that experimental conditions of powder preparation, electric field and stirring, have a marked effect on suspension stability. The microstructure of the coatings is influenced by particle morphology and electric field. Zeta potential measurements revealed an ageing effect. The deposit yield has been quantified with respect to deposition duration and applied voltage. SEM observations revealed partial densification of coatings consisting of submicrometre HA particles after thermal treatment at 930 °C.

References

1. P. DUCHEYNE, L. L. HENCH, A. KAGAN II, M. MARTENS, A. BURSENS and J. C. MULIER, *J. Biomed. Mater. Res.* **14** (1980) 225.
2. D. P. RIVERO, J. FOX, A. K. SKIPOR, R. M. URBAN and J. O. GALANTE, *ibid.* **22** (1988) 191.
3. S. D. COOK, J. F. KAY, K. A. THOMAS and M. JARCHO, *J. Oral Maxillof. Implants* **2** (1987) 15.
4. P. DUCHEYNE, W. VAN RAEMDONCK, J. C. HEUGHEBAERT and M. HEUGHEBAERT, *Biomaterials* **7** (1986) 97.
5. P. DUCHEYNE, S. RADIN, M. HEUGHEBAERT and J. C. HEUGHEBAERT, *ibid.* **11** (1990) 244.
6. C. S. KIM and P. DUCHEYNE, *ibid.* **12** (1991) 461.
7. T. UMEGAKI, K. YAMASHITA and T. KANAZAWA, *Memoirs of Faculty of Technol. Tokyo Metropolitan Univ.* **38** (1988) 4003.
8. A. STOCH and A. BROZEK, *Third Euro-Ceramics* **3** (1993) 75.
9. R. DAMODARAN and B. M. MOUDGIL, *Colloids and Surfaces A*: *Physicochem. Engng Aspects* **80** (1993) 191.
10. T. UMEGAKI, Y. HISANO, K. YAMASHITA and T. KANAZAWA, *Gypsum & Lime* **218** (1989) 24.
11. F. HARBACH, R. NEEFF, H. NIENBURG and L. WEILER, in Proceedings of 2nd International Conference on Ceramic Powder Processing Science, edited by H. Hausner, G. L. Messing and S. Hirano (Dtsch. Keram. Ges.: Cologne, Germany, 1988) p. 609.
12. R. NASS, W. STORCH, H. SCHMIDT, F. HARBACH, R. NEEFF and H. NIENBURG in Proceedings of 2nd International Conference on Ceramic Powder Processing Science, edited by H. Hausner, G. L. Messing and S. Hirano (Dtsch. Keram. Ges., Cologne, Germany, 1988) p. 625.
13. L. GAR-OR, S. LIUBOVICH and S. HABER, *J. Electrochem. Soc.* **139** (1992) 1078.
14. M. JARCHO, C. H. BOLEN, M. B. THOMAS, J. BOBICK, J. F. KAY and R. H. DOREMUS, *J. Mater. Sci.* **11** (1976) 2027.
15. K. ISHIKAWA, M. KON, S. TENSHIN, Y. ISHIKAWA and N. KUWAYAMA, *Chemistry Express* **5** (1990) 725.
16. J. MIZUGUCHI, K. SUMI and T. MUCHI, *J. Electrochem. Soc.* **130** (1983) 1819.
17. P. DUCHEYNE, C. S. KIM and S. R. POLLACK, *J. Biomed. Mater. Res.* **26** (1992) 147.
18. M. KAGAWA, Y. SYONO, Y. IMAMURA and S. USUI, *J. Amer. Ceram. Soc.* **69** (1986) C50.
19. J. H. KENNEDY and A. FOISSY, *ibid.* **60** (1977) 33.
20. M. J. SHANE, J. B. TALBOT, B. G. KINNEY, E. SLUZKY and K. R. HESSE, *J. Colloid Interface Sci.* **165** (1994) 334.
21. J. K. G. PANITZ, M. T. DUGGER, D. E. PEEBLES, D. R. TALLANT and C. R. HILLS, *J. Vac. Sci. Technol.* **A11** (1993) 1441.
22. Y. ZHANG, C. J. BRINKER and R. M. CROOKS, *Mater. Res. Soc. Symp. Proc.* **271** (1992) 465.
23. R. W. POWERS, Amer. Ceram. Soc. Bull. **65** (1986) 1270.
24. *Idem., J. Electrochem. Soc.* **122** (1975) 490.
25. D. E. CLARK, W. J. DALZELL and D. C. FOLZ, *Ceram. Engng. Sci. Proc.* **9** (1988) 1111.
26. J. M. ANDREWS, A. H. COLLINS, D. C. CORNISH and J. DRACASS, *Proc. Brit. Ceram. Soc.* **12** (1969) 211.
27. F. LINDNER and A. FELTZ, *J. Europ. Ceram. Soc.* **11** (1993) 269.
28. *Idem., Solid State Ionics* **63–65** (1993) 13.
29. E. V. KOROBKO, in Proceedings of the Conference on Recent Advances in Adaptive and Sensory Materials and Their Applications, Blacksburg, Virginia, edited by C. A. Rogers and R. C. Rogers (Technomic 1992) p. 3.
30. W. A. PLISKIN and E. E. CONRAD, *J. Electrochem. Technol.* **2** (1964) 196.
31. R. J. BROOK, *Proc. Brit. Ceram. Soc.* **32** (1982) **7**.
32. H. HAHN, J. LOGAS and R. S. AVERBACK, *J. Mater. Res.* **5** (1990) 609.
33. S. BEST, W. BONFIELD, *J. Mater. Sci. Mater. Med.* **5** (1994) 516.
34. C. CHAI, B. BEN-NISSAN, S. PYKE and L. EVANS, *Mater. Manuf. Processes* **10** (1995) 205.
35. A. CIGADA, M. CABRINI and P. PEDEFERRI, *J. Mater. Sci. Mater. Med.* **3** (1992) 408.

Received 18 December 1995
and accepted 18 September 1996